ELSEVIER

Journal of Hazardous Materials B93 (2002) 167–186

Journal of Hazardous Materials

www.elsevier.com/locate/jhazmat

Stabilization of phosphogypsum using class C fly ash and lime: assessment of the potential for marine applications

Kelly A. Rusch*, Tingzong Guo, Roger K. Seals

Department of Civil and Environmental Engineering, Louisiana State University, Baton Rouge, LA 70803, USA

Received 12 January 2000; received in revised form 7 November 2001; accepted 28 November 2001

Abstract

Phosphogypsum (PG, $CaSO_4 \cdot H_2O$), a solid byproduct of phosphoric acid manufacturing, contains low levels of radium (^{266}Ra), resulting in stackpiling as the only currently allowable disposal/storage method. PG can be stabilized with class C fly ash and lime for potential use in marine environments. An augmented simplex centroid design with pseudo-components was used to select 10 PG:class C fly ash:lime compositions. The 43 cm^3 blocks were fabricated and subjected to a field submergence test and 28 days saltwater dynamic leaching study. The dynamic leaching study yielded effective calcium diffusion coefficients (D_e) ranging from 1.15×10^{-13} to 3.14×10^{-13} $m^2\ s^{-1}$ and effective diffusion depths (X_c) ranging from 14.7 to 4.3 mm for 30 years life. The control composites exhibited diametrical expansions ranging from 2.3 to 17.1%, providing evidence of the extent of the rupture development due to ettringite formation. Scanning electron microscopy (SEM), microprobe analysis showed that the formation of a $CaCO_3$ on the composite surface could not protect the composites from saltwater intrusion because the ruptures developed throughout the composites were too great. When the PG:class C fly ash:lime composites were submerged, saltwater was able to intrude throughout the entire composite and dissolve the PG. The dissolution of the PG increased the concentration of sulfate ions that could react with calcium aluminum oxides in class C fly ash forming additional ettringite that accelerated rupture development. Effective diffusion coefficients and effective diffusion depths alone are not necessarily good indicators of the long-term survivability of PG:class C fly ash:lime composites. Development of the ruptures in the composites must be considered when the composites are used for aquatic applications. © 2002 Elsevier Science B.V. All rights reserved.

Keywords: Phosphogypsum; Stabilization; Aquatic application; Class C fly ash; Lime

* Corresponding author. Tel.: +1-225-3888528; fax: +1-225-3888662.
E-mail address: krusch@lsu.edu (K.A. Rusch).

0304-3894/02/$ – see front matter © 2002 Elsevier Science B.V. All rights reserved.
PII: S0304-3894(02)00009-2

1. Introduction

Phosphoric acid production in the United States uses the wet process in which the phosphorous is extracted from the ore with sulfuric acid. This process, while low in cost, results in the significant production of the solid byproduct phosphogypsum (PG, $CaSO_4 \cdot 2H_2O$). PG is a moist gray, powdery, acidic (pH = 2–3) material containing residual acid, fluoride, toxic metals and radionuclides [1]. Of particular concern is radium (^{266}Ra) which is present at concentrations about tens of times background soil levels [2,3]. ^{266}Ra decays to radon gas having a half-life of 3.8 days. Radon's further decay releases α particles, which can potentially cause cancer if ingested. Subsequently, the United States Environmental Protection Agency has classified ^{266}Ra as a Group A, human carcinogen that has resulted in the regulated disposal/usage of PG under the National Emission Standards for Hazardous Air Pollutants (NESHAP) and the National Emissions Standards for Radon Emission from PG Stacks [4,5]. The current allowable disposal method for PG is stackpiling, resulting in the creation of at least 33 stacks with an average area of 0.91 km^2 per stack [6].

As a general rule, 4.5 metric tonnes of PG are generated for every metric ton of phosphoric acid produced [7], resulting in an annual PG generation rate of approximately 32 million metric tonnes in the states of Florida, Louisiana and Texas [1]. Total accumulations are well in excess of 720 million metric tonnes, causing significant space and environmental problems and placing increasing pressure on the fertilizer industry to find long-term solutions [8]. While research is being conducted to find applications for this byproduct material, the radioactivity and acidity of PG detract from its wide-spread use. One area that does show promise is aquatic applications that would virtually eliminate the airborne vector of transmission for radon. Bioaccumulation up the food chain would be the only source of potential radon exposure.

Recent research at Louisiana State University indicated that Portland cement-stabilized PG provided a good foundation for marine organism growth [9]. However, the composites used in this study contained 30% Portland type I cement, an order of magnitude higher than that considered to be economically feasible for aquatic applications [10]. Further research [11–13] has shown that composite stability under saltwater conditions is dependent on the development of a calcium carbonate ($CaCO_3$) coating on the composite surface to protect the PG from dissolving which has a saltwater solubility of approximately 4 $g\,l^{-1}$ [14]. The catalyst affecting the presence or absence of the $CaCO_3$ coating on the composite surface was determined to be a localized zone of high pH [12].

Preliminary economic analyses indicated the cement content must be less than 5% to produce stabilized PG composites that are economically competitive with current materials used in coastal applications [10]. However, at this level, cement alone will not provide enough binding and neutralizing capacity to maintain the physical integrity of the composites under saltwater conditions [12]. Thus, low cost admixtures that can neutralize the acidic nature of PG and provide cementous binding properties are required.

This paper presents the results of studies investigating the use of class C fly ash and lime as binding and neutralizing agents in PG stabilization. Varying PG:class C fly ash:lime composites were fabricated and subjected to laboratory dynamic leaching and field submergence

tests to determine an appropriate mixture that had the potential to maintain long-term physical integrity under saltwater conditions.

2. Materials and methods

2.1. Admixture experimental design

There are two essential conditions affecting the survival of stabilized PG composites in the saltwater environment. First, the local pH environment on the composite surface should be high enough to promote the precipitation and formation of a $CaCO_3$ layer that seals and protects the block from saltwater intrusion [15]. Second, the composite should be strong enough to resist current, wave and other external forces in the marine environments. Admixtures of class C fly ash and lime were selected to address these conditions. Fly ash, a solid byproduct from coal combustion in electric power plants, is composed of metallic oxides, silicates and other particulate matter. The exact chemical composition is influenced by the type of coal used, the completeness of the combustion process, and the mineral content of the coal [16]. Class C fly ash was selected over class F ash because it contains high levels of calcium and silicon recovered as oligomeric silicates from hydration products, providing good neutralizing and cementing capabilities [17,18]. The fly ash can provide both binding and neutralizing capacity for the PG composites. Lime was selected to provide additional neutralizing capacity and to assure localized pH values greater than 10 required for $CaCO_3$ formation [15].

An augmented simplex centroid design with pseudo-components method was used to select 10 composite combinations (Table 1) and to ensure a better distribution of information throughout the experimental region. The pseudo-components method [19,20] was used to ensure that all three components (PG, class C fly ash and lime) were represented in some minimum proportions, having lower bounds (L_i) that are constrained by: $0 < L_i < x_i < 1$ with PG (x_1), class C fly ash (x_2), and lime (x_3) and ($L_1 = 0.55$, $L_2 = 0.35$, $L_3 = 0.03$).

Table 1
Ten PG:class C fly ash:lime ingredients compositions (%) were selected using the augmented simplex centroid design with pseudo-components and fabricated under a static pressure of 9.8×10^7 N m^{-2}

PG (%)	Class C fly ash (%)	Lime (%)
62.0	35.0	3.0
58.5	38.5	3.0
55.0	42.0	3.0
59.6	36.2	4.2
56.2	39.6	4.2
57.4	37.3	5.3
58.5	35.0	6.5
55.0	38.5	6.5
56.2	36.2	7.6
55.0	35.0	10.0

The pH of all 10 mixture combinations was above 10 to ensure that calcium carbonate would precipitate on the surface of the PG blocks [12].

2.2. Fabrication

Dried lime, class C fly ash and ground, dried PG (passed through a 2 mm sieve) were combined, homogenized and mixed with water equivalent to 8% of dry weight (mass of water/mass of dry solid = 8%). A 96 g of the resulting mixture were poured into a 38 mm diameter steel mold and compacted into a 38 mm long cylinder under 9.8×10^7 N m^{-2} pressure using a static press. The composites were allowed to cure at room temperature and 100% humidity for over 2 weeks before testing. The mean mass of all composites was 87 g, resulting in a solid density of 2.0 g cm^{-3}.

2.3. Experimental treatments

PG composites within each composition were divided into three groups. Group one was stored in sealed, plastic bags and did not receive any treatment (control group). Group two was submerged in a natural saltwater bay located in Grand Isle, Louisiana. Group three was subjected to 28 days dynamic leaching test.

Composite diameters (ϕ) of the control group were measured using a caliper at $t = 1$ and 300 days (10 months) after block fabrication. The $t = 300$ days blocks were kept in plastic bags up to the time of measurement.

$$\alpha = \frac{\phi_{10\,\text{months}} - \phi_{1\,\text{day}}}{\phi_{1\,\text{day}}} \tag{1}$$

The measured diameters were used to calculate percent diameter expansion (α). Increases in block diameter over time provide some indication of potential ettringite formation [21]:

$$3\text{CaO} \cdot \text{Al}_2\text{O}_3 + 3(\text{CaSO}_4 \cdot 2\text{H}_2\text{O}) + 26\text{H}_2\text{O} \rightarrow 3\text{CaO} \cdot \text{Al}_2\text{O}_3 \cdot 3\text{CaSO}_4 \cdot 32\text{H}_2\text{O} \tag{2}$$

The formation of the ettringite results in a volume increase of 227% [22]. However, there is little room for expansion before ruptures develop due to the high composite density (2.0 g cm^{-3}).

Saltwater submergence tests were conducted to evaluate the impact of the natural marine environment on the PG composites. Four blocks from each composition were randomly selected, randomly positioned (two per frame), and securely suspended with tie wrap and monofilament in a frame and fully submersed in the bay adjacent the Louisiana Sea Grant Grand Isle Bivalve Culture Facility. The temperature and salinity of the saltwater ranged from 16 to 31 °C and 17 to 29‰, respectively. The physical condition (diameter, length and degradation) of the composites was monitored at 3 weeks intervals.

A variation of the dynamic leaching test [23] was performed in duplicate to determine calcium release rates as an indicator of potential composite dissolution. The composites were placed in 20‰ artificial saltwater (Instant Ocean^{TM}) at a leachate volume to composite

surface area ratio of 8:1. The leachate, completely exchanged at intervals of 0.08, 0.29, 1–5, 8, 11, 14, 21, and 28 days to prevent saturation of the solution, was analyzed for calcium by ICP in accordance with standard methods [24].

2.4. Data analyses

Research by Guo [11] indicated that the reactants, Ca^{2+} and $CO_3{}^{2-}$, for the formation of the $CaCO_3$ coating on the PG composite surface originated from saltwater and not from the PG composite. Thus, Ca^{2+} release from the PG composite can be considered non-reactive, allowing for the use of the effective diffusion coefficient [25]. The diffusive flux of calcium ions can be estimated by Fick's second law [26]:

$$\frac{\delta C}{\delta t} = D_e \frac{\delta^2 C}{\delta x^2}, \qquad 0 \le x \le \infty, \quad 0 \le t \tag{3}$$

where C (mol cm^{-3}) is the concentration of calcium ions in the composite, t (days) the time, D_e (cm^2 per day) the effective diffusion coefficient, x (cm) is the one-dimensional coordinate. The original point ($x = 0$) is on the composite surface with movement into the composite extending from $x = 0$ to $+\infty$. The model assumes a uniform distribution of calcium ions within the composite and a flux of the ions across the composite-water interface that is proportional to the concentration at the composite interface. For a well-stirred aqueous system, the boundary conditions are therefore [26]:

$$\text{at} \quad t = 0, \quad C = C_0 \tag{4}$$

$$\text{at} \quad x = 0, \quad C = 0 \tag{5}$$

where C_0 is the initial concentration of calcium ions in the composite. For the condition when

$$t \gg \frac{D_e}{h} \tag{6}$$

where

$$h = \frac{D_e \partial C}{C \partial x} \tag{7}$$

the solution for Eq. (3) is

$$J = C_0 \sqrt{\frac{D_e}{\pi t}} \tag{8}$$

where J (mol cm^{-2} per day) is the flux of calcium ions. Eq. (8) can be rewritten in its log–log form as

$$\log(J) = -0.5 \log(t) + \log(C_0) + 0.5 \log(D_e) - 0.5 \log(\pi) \tag{9}$$

which indicates that if $\log(J)$ values are regressed against $\log(t)$, the slope of the line should be -0.5 for diffusion controlled processes and can be used to verify the assumptions for the model. Eq. (9) also indicates that

$$\text{intercept} = \log(C_0) + 0.5 \log(D_e) - 0.5 \log(\pi) \tag{10}$$

which can then be used to calculate the effective diffusion coefficient. This model is widely used for estimation of effective diffusion coefficients because it is simple, reliable and self-verified [27,28]. The effective diffusion depth, X_c (cm), defined as the depth at which the Ca^{2+} concentration changes due to diffusion, is given by [26]:

$$X_c = \sqrt{2D_e t} \tag{11}$$

Eqs. (10) and (11) were used to calculate the effective diffusion coefficients and effective diffusion depths for PG:class C fly ash:lime composites based on data collected from dynamic leaching study.

2.5. Microscopy analysis

Qualitative and quantitative X-ray microprobe (Joel JXA-733) analyses and scanning electron microscopy (SEM Joel 8408) were used to analyze the microstructure of the control composites and composites subjected to dynamic leaching tests. Specifically, observations were made to determine the presence of ettringite and the $CaCO_3$ coating. Three PG composites with typical ingredient combinations; 62%:35%:3%, 55%:42%:3% and 58.5%:35%:6.5% PG:class C fly ash:lime, were selected based on the degree of surface degradation. This excluded the most fragile composites since they were too soft to be

Table 2
Rupture widths and diameters were measured for the control group

PG (%)	Class C fly ash (%)	Lime (%)	ϕ (mm)	Mean ϕ (mm)	Mean α (%)	Rupture width ± S.D. (mm)	Mean rupture width (mm)
62.0	35.0	3.0	39.0	39.0	2.3	0.009 ± 0.001	0.01
62.0	35.0	3.0	39.0			NA	
58.5	38.5	3.0	39.3	39.3	3.2	NA	NA
58.5	38.5	3.0	39.3			NA	
55.0	42.0	3.0	39.9	39.9	4.7	0.039 ± 0.003	0.039
55.0	42.0	3.0	39.9			NA	
59.6	36.2	4.2	41.3	41.4	8.7	0.874 ± 0.03	0.874
59.6	36.2	4.2	41.5			0.874 ± 0.05	
56.2	39.6	4.2	40.7	40.7	6.8	0.784 ± 0.02	0.775
56.2	39.6	4.2	40.7			0.766 ± 0.01	
57.4	37.3	5.3	40.4	40.4	6.0	1.26 ± 0.06	1.19
57.4	37.3	5.3	40.4			1.12 ± 0.08	
58.5	35.0	6.5	42.5	42.5	11.6	1.70 ± 0.13	1.78
58.5	35.0	6.5	42.5			1.86 ± 0.10	
55.0	38.5	6.5	43.0	43.1	13.1	1.54 ± 0.08	1.53
55.0	38.5	6.5	43.2			1.52 ± 0.10	
55.0	38.5	7.6	41.4	41.4	8.9	2.14 ± 0.08	2.19
55.0	38.5	7.6	41.4			2.24 ± 0.08	
55.0	35.0	10.0	44.5	44.6	17.1	2.70 ± 0.10	2.77
55.0	35.0	10.0	44.7			2.84 ± 0.26	

Percent diametrical expansions were also calculated for the control group (initial diameter of the PG composite was 38 mm).

prepared for microprobe analysis. The 30 μm sections from the selected composites were prepared according to standard thin section method [29].

Rupture width was measured with a caliper. The ruptures contained in the composites with 3% lime were too small for caliper measurement therefore their backscatter images were used to estimate the rupture width. The rupture widths are the averages of all five measurements per composite.

3. Results

3.1. Diameter of PG composites and rupture measurements

There is a positive linear relationship between lime content and composite diameter for the control group (Table 2 and Fig. 1).

$$\phi\,(\text{mm}) = 0.7356 \times \text{lime}\,(\%) + 37.39, \qquad r^2 = 0.863 \tag{12}$$

However, no clear trend exists between composite diameter and class C fly ash for a given lime content. It was also found that after 10 months of air curing (control condition), visible

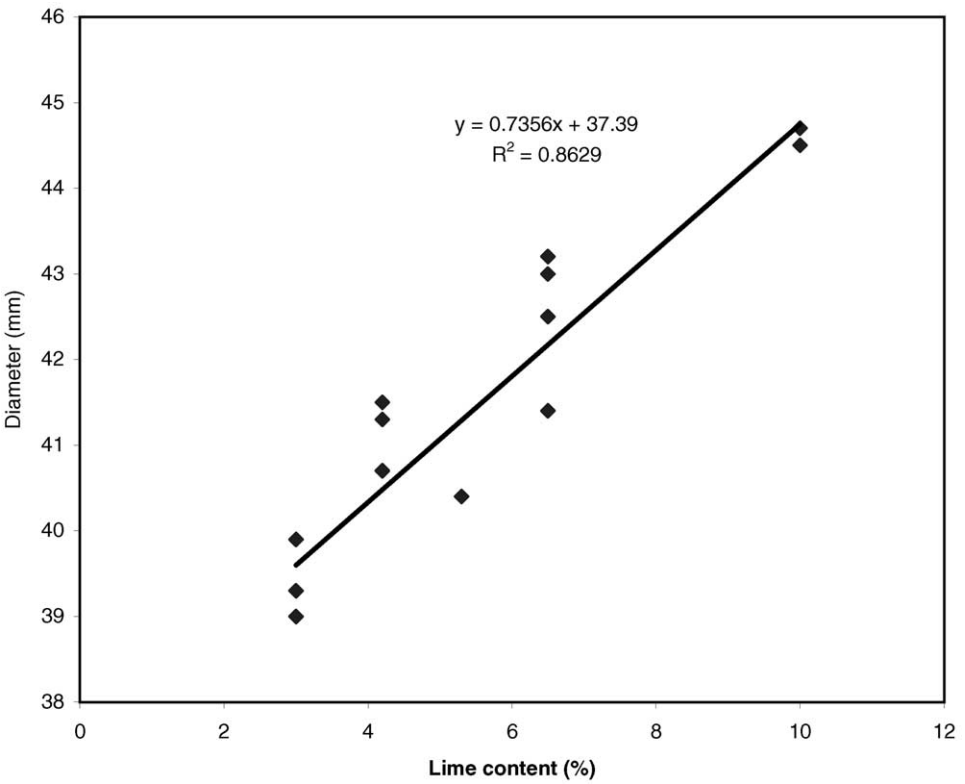

Fig. 1. The plot of composite diameter vs. lime content indicated a positive relationship between diameter and lime content.

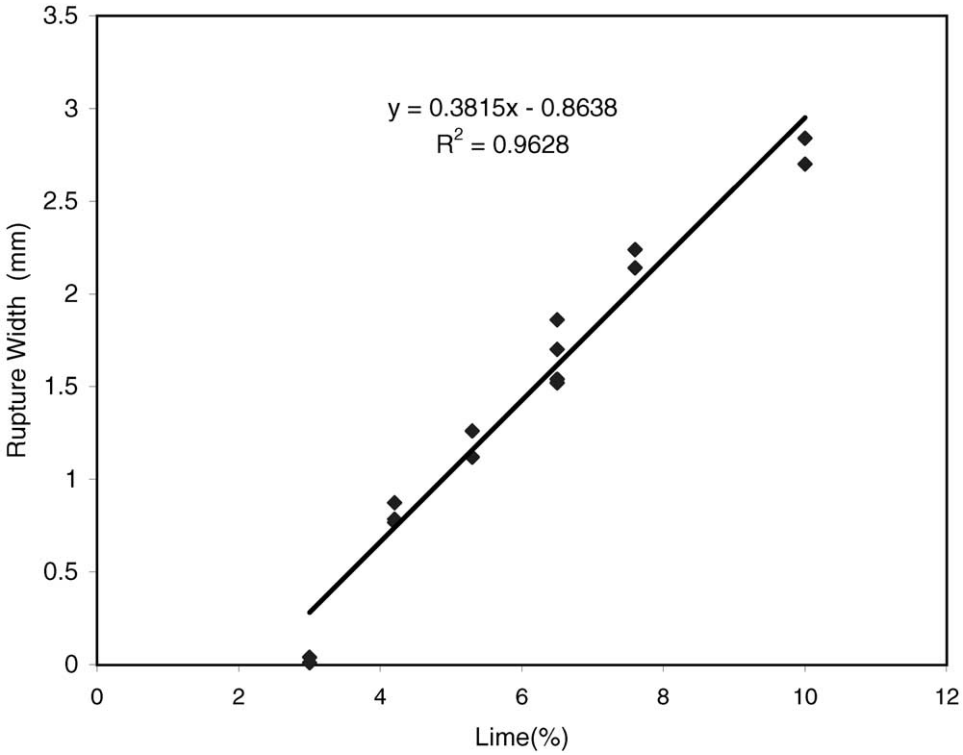

Fig. 2. The plot of rupture composite width vs. lime content indicated a positive relationship between rupture width and lime content.

ruptures (>1 mm) developed on the surfaces of all of the composites having a lime content greater than 5.3% (Table 2). Similar ruptures were observed in the leached samples. As lime content increased, the rupture width of the control PG composites increased linearly (Fig. 2).

$$\text{rupture width (mm)} = 0.3815 \times \text{lime (\%)} - 0.8638, \qquad r^2 = 0.963 \tag{13}$$

However, there is no clear trend between rupture width and class C fly ash for a given lime content.

3.2. Field saltwater submergence observations and percent diameter expansion

Within the first 3 weeks of submergence, the composites were already exhibiting surface ruptures (Fig. 3). At 6th week, erosion of the edges was observed. This erosion continued (as long as 15 weeks) until all of the composites had deteriorated to the point that they fell off of the frame and were lost to the surrounding environment. The percent diameter expansion ranged from 2.3 to 17.1%.

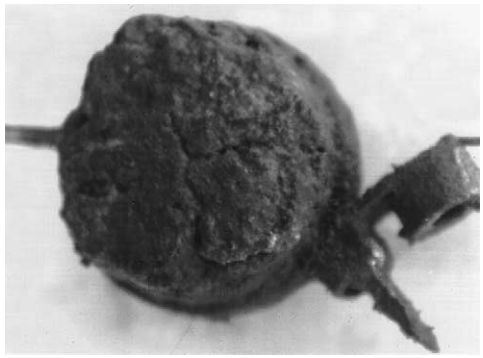

Fig. 3. The 58.5%:35%:6.5% PG:class C fly ash:lime composite exhibited severe degradation after 6 weeks saltwater submergence.

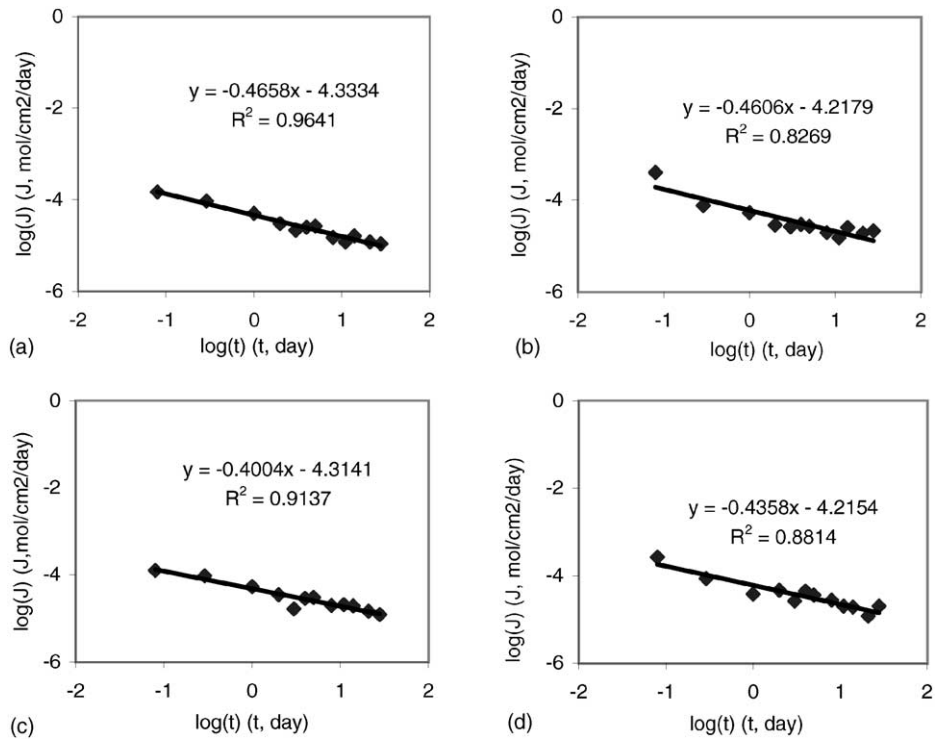

Fig. 4. The flux of Ca^{2+} from PG:class C fly ash:lime composite during the dynamic leaching study indicated that Ca^{2+} release is diffusion driven. (a) 62%:35%:3% PG:class C fly ash:lime composite, (b) 58.5%:35%:6.5% PG:class C fly ash:lime composite, (c) 58.5%:38.5%:3% PG:class C fly ash:lime composite, (d) 56.2%:39.6%:4.2% PG:class C fly ash:lime composite.

3.3. Calcium diffusion coefficients and effective diffusion depth

Illustrative log–log plots of $J(Ca^{2+})$ versus time are presented for several lime levels (Fig. 4). All 10 composite combinations resembled the plots shown in Fig. 4. Based on Eq. (8), slopes of the regression equation should equal −0.5 if diffusion is the dominant mechanism responsible for Ca^{2+} leaching. Statistical analyses ($\alpha = 0.05$) indicate that only four composites failed to meet the null hypothesis of a diffusion slope of −0.5 (Table 3). Both replicates of the 58.5%:38.5%:3.0% PG:class C fly ash:lime composite (slope = 0.35–0.39) failed to meet the null hypothesis, while one replicate of the 56.2%:39.6%:4.2% PG:class C fly ash:lime (slope = 0.37) and 55.5%:35.5%:6.5% PG:class C fly ash:lime (slope = 0.37) composites failed to meet the null hypothesis. D_e ranged from 1.15×10^{-13} to 3.14×10^{-13} $m^2\ s^{-1}$, while X_c ranged from 14.7 to 24.3 mm for 30 years submergence.

3.4. SEM and microprobe analyses

Surface zone SEM images of the leached 62%:35%:3% PG:class C fly ash:lime composite show a 20 μm loose layer of $CaCO_3$ embedded with spherical class C fly ash particles and surrounding a 10 μm wide rupture (Fig. 5a–c). These images also show that ruptures developed across the $CaCO_3$ layer and that no PG crystals were present. The body zone

Table 3
The slopes and intercepts of log–log plots of $J(Ca^{2+})$ vs. time for the composites subjected to the 28 days dynamic leaching study indicate that most of the PG:class C fly ash:lime composites observe the theoretical diffusion process (slope = −0.5)

PG (%)	Class C fly ash (%)	Lime (%)	Intercept	Slope	S.D. for slope	H_0: slope = −0.5, H_a: slope ≠ −0.5, *t*-value	Conclusion (α=0.05)
62.0	35.0	3.0	−4.29	–0.506	0.027	−0.24	Accept H_0
62.0	35.0	3.0	−4.33	−0.466	0.028	1.20	Accept H_0
58.5	38.5	3.0	−4.31	−0.400	0.039	2.56	Accept H_a
58.5	38.5	3.0	−4.33	−0.403	0.035	2.80	Accept H_a
55.0	42.0	3.0	−4.38	−0.421	0.036	2.19	Accept H_0
55.0	42.0	3.0	−4.35	−0.388	0.060	1.88	Accept H_0
59.6	36.2	4.2	−4.32	−0.457	0.16	0.27	Accept H_0
59.6	36.2	4.2	−4.21	−0.444	0.070	0.79	Accept H_0
56.2	39.6	4.2	−4.22	−0.436	0.051	1.27	Accept H_0
56.2	39.6	4.2	−4.26	−0.367	0.050	2.69	Accept H_a
57.4	37.3	5.3	−4.30	−0.407	0.071	1.30	Accept H_0
57.4	37.3	5.3	−4.21	−0.468	0.090	0.35	Accept H_0
58.5	35.0	6.5	−4.22	−0.461	0.067	0.59	Accept H_0
58.5	35.0	6.5	−4.29	−0.424	0.066	1.15	Accept H_0
55.0	38.5	6.5	−4.41	−0.372	0.077	2.24	Accept H_a
55.0	38.5	6.5	−4.36	−0.418	0.093	0.88	Accept H_0
56.2	36.2	7.6	−4.34	−0.736	0.15	−1.55	Accept H_0
56.2	36.2	7.6	−4.39	−0.692	0.22	−0.89	Accept H_0
55.0	35.0	10.0	−4.41	−0.375	0.15	0.81	Accept H_0
55.0	35.0	10.0	−4.34	−0.382	0.11	1.06	Accept H_0

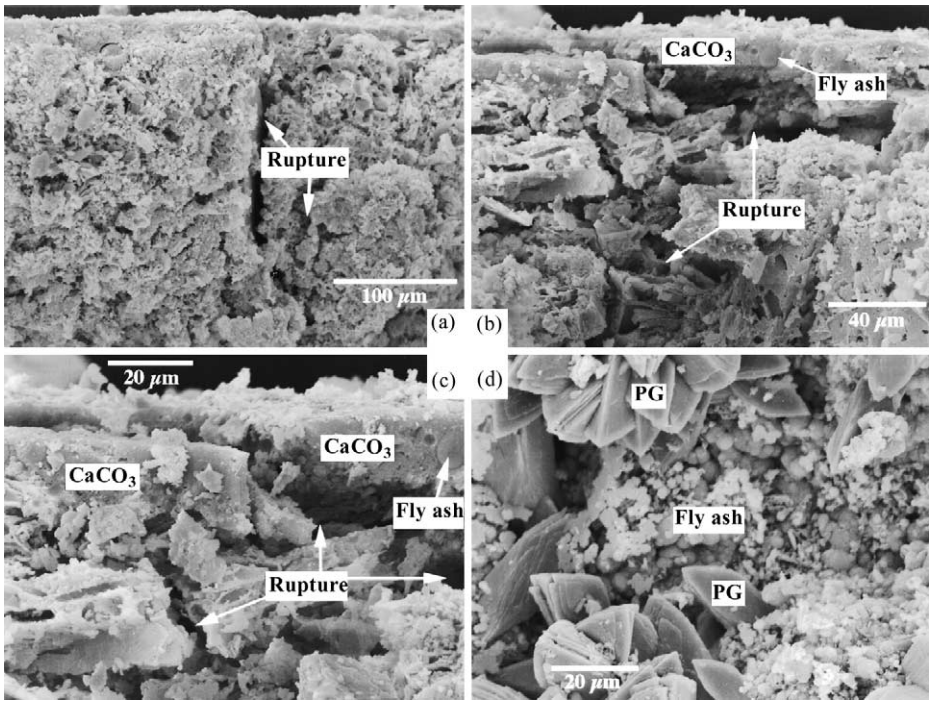

Fig. 5. SEM images of the 62%:35%:3% PG:class C class C fly ash:lime composite after 28 days saltwater dynamic leaching test showed rupture development. (a) The 10 μm ruptures were found on the composite surface zone. (b) A dense layer of $CaCO_3$ embedded with spherical class C fly ash particles was found on the composite surface. This 20 μm layer was broken and formed over a 10 μm wide rupture. (c) The surface zone image showed clear details of $CaCO_3$ layer, spherical class C fly ash particles and ruptures. (d) The body of the composite contained plate crystal PG mixed with spherical class C fly ash particles.

image (Fig. 5d) of the same composite shows homogeneously mixed PG and class C fly ash, and all class C fly ash particle surfaces were covered with a new layer of crystals.

The SEM images of the control 62%:35%:3% PG:class C fly ash:lime composite surface show exposed PG and class C fly ash particles (Fig. 6a–c). In some areas, a 5–15 μm layer of paste covers the PG surface, and 1 μm wide ruptures developed throughout the composite. The composite body image (Fig. 6d) revealed the formation of ettringite, which was identified based on work performed by Roy et al. [30].

SEM images (Fig. 7a–c) of the surface zone of the leached 55%:42%:3% PG:class C fly ash:lime composite show a 10 μm loose layer of $CaCO_3$ embedded with spherical class C fly ash particles. The body of the same composite contained newly formed PG crystals on the spherical fly ash particles (Fig. 7d). The SEM images of the 55%:42%:3% PG:class C fly ash:lime control composite were similar to those from the 62%:35%:3% composite.

SEM images (Fig. 8a and b) of the surface zone of the leached 58.5%:35%:6.5% PG:class C fly ash:lime composite show the development of 50 μm wide ruptures on the composite surface. The surface was loose and easily removed. The composite body contained

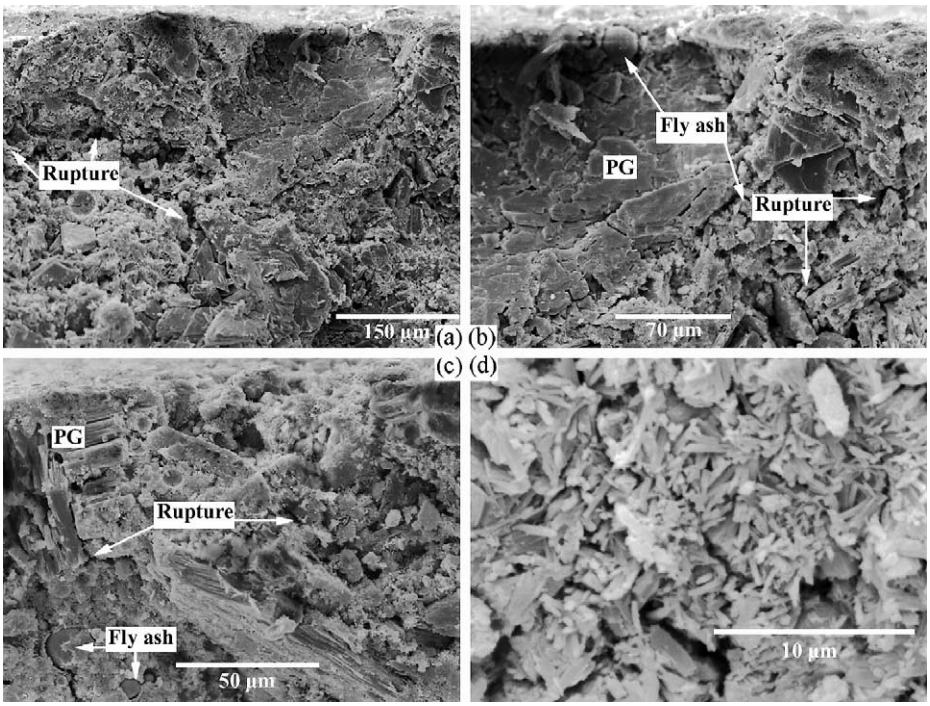

Fig. 6. SEM images of the 62%:35%:3% PG:class C fly ash:lime composite after a 10 months air curing showed rupture development. (a) Ruptures were clearly developed throughout the surface zone. (b) The surface contained spherical class C fly ash particles, plate crystal PG and ruptures. (c) Plate crystal PG was exposed on the surface of the composite. (d) The body of the composite contained plate crystal PG mixed with spherical class C fly ash particles.

homogeneously mixed PG and class C fly ash. All of the fly ash particles were covered with a layer of gypsum crystals that were identified through X-ray qualitative analysis (Fig. 8c and d). The 58.5%:35%:6.5% PG:class C fly ash:lime control composite exhibited similar characteristics as the 62%:35%:3% control composite. The only difference is the development of 20 μm wide ruptures throughout the composite.

The back-scattered (BS) electron images of the 62%:35%:3% PG:class C fly ash:lime (Fig. 9a), 55%:42%:3% PG:class C fly ash:lime (Fig. 9b) and the 58.5%:35%:6.5% PG:class C fly ash:lime (Fig. 9c) composites show that there are 50 μm wide ruptures along the surface. The BS electron image and X-ray elemental content images of calcium (Ca), silicon (Si), sulfur (S) and aluminum (Al) for 62%:35%:3% PG:class C fly ash:lime composite surface zone are presented in Fig. 10. The BS image shows that some spherical class C fly ash particles exist in the surface zone. The calcium content image illustrates a high calcium content zone along the PG composite surface, but the high calcium content region is not uniform. It randomly includes some low calcium content spots. The aluminum content image shows that in the high calcium content regions, low calcium spots correspond to high aluminum content areas. The silicon content image shows that in high calcium content

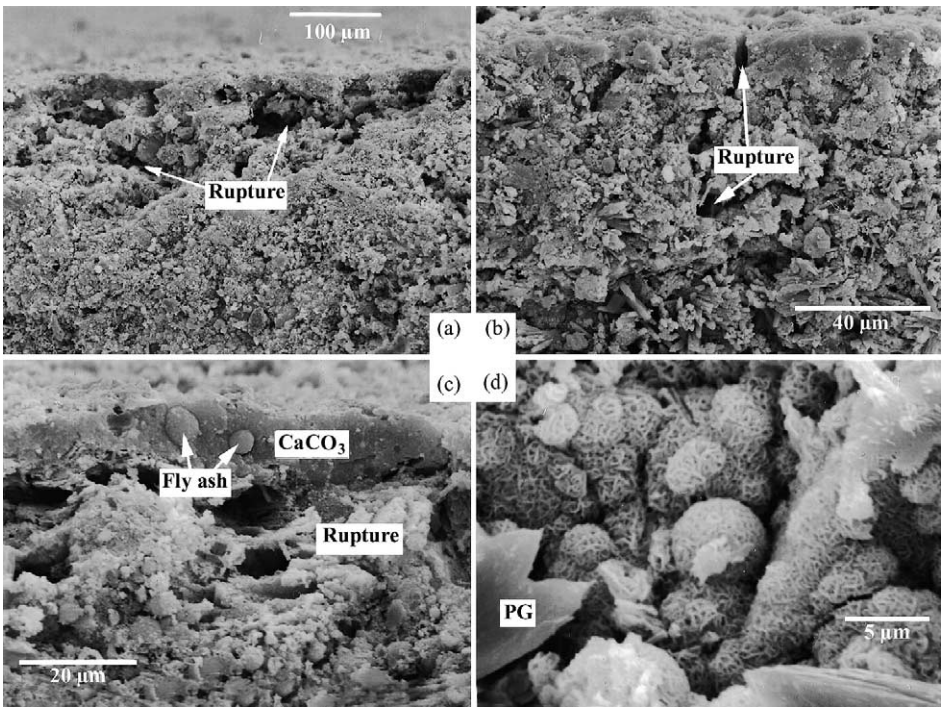

Fig. 7. SEM images of the 55%:42%:3% PG:class C fly ash:lime composite after 28 days saltwater dynamic leaching test showed rupture development. (a) The 40 μm ruptures were found on the composite surface zone. (b) The 10 μm ruptures were found on the composite surface zone. (c) A dense layer of $CaCO_3$ embedded with spherical class C fly ash particles was found on the composite surface. This 10 μm thick layer was broken and formed over a 40 μm wide rupture. (d) Newly formed crystals were found on the spherical class C fly ash surface within the body of the composite. These crystals were identified to be composed of S, O and Ca.

regions, the low calcium spots correspond to high aluminum content area. The silicon content image also shows that in low calcium content regions, silicon content is continuous and shows spherical shapes in places. The magnesium content image shows that a higher magnesium contents exists between the $CaCO_3$ coating and composite. The sulfur content image indicates that no sulfur exists in the PG composite surface. The BS and elemental content images of 58.5%:35%:6.5% PG:class C fly ash:lime (Fig. 11) have similar distribution patterns for calcium, aluminum, magnesium, silicon, sulfur and BS.

4. Discussion

When the PG:class C fly ash:lime composites were fabricated, the pozzolanic reaction between class C fly ash and lime resulted in the formation of a hard paste [31,32]. Over time, and in the presence of PG, the pozzolanic reaction continued and the development and modification of ettringite and other calcium silicate hydrate products led to the expansion

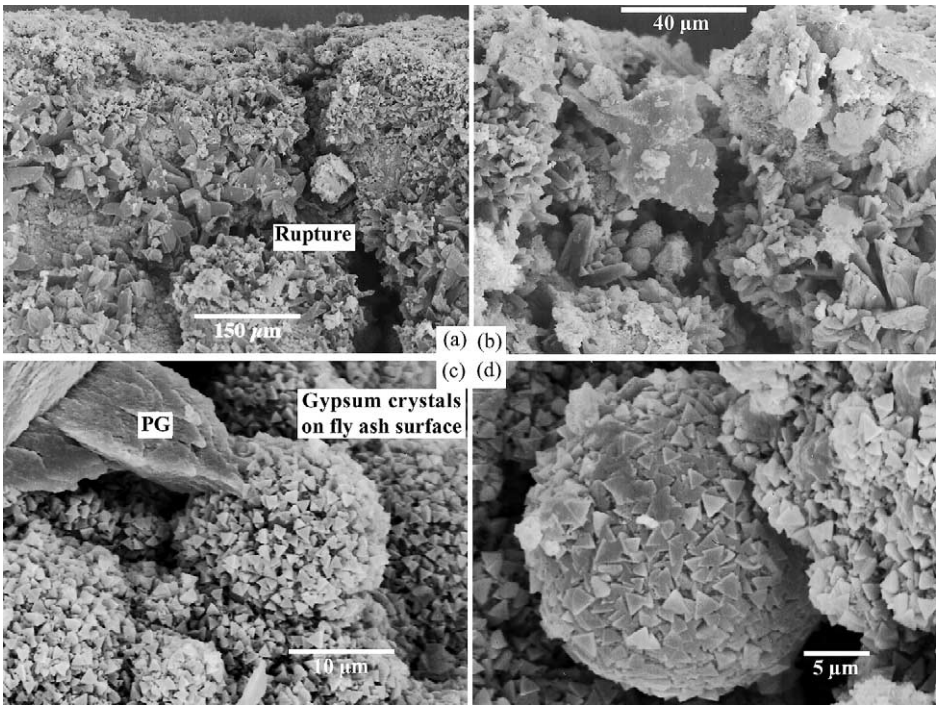

Fig. 8. SEM images of the 58.5%:35%:6.5% PG:class C fly ash:lime composite after 28 days saltwater dynamic leaching test showed rupture development and newly formed gypsum. (a) The 50 μm ruptures were found on the composite surface zone. (b) Details of the rupture in Fig. 5a. (c) Newly formed gypsum crystals were found on all spherical class C fly ash particles. (d) Details of newly formed gypsum crystals on a spherical class C fly ash particle.

of the harden paste [31,32]. A theoretical maximum percent diametrical expansion, $\alpha_{max} = 1.8\%$, was determined from similar research focused on PG:class C fly ash:Portland type II cement composites [11]. All percent diametrical expansions for the PG:class C fly ash:lime composites were greater than the threshold selected. This resulted in ruptures developing before the PG composites were submerged in the saltwater, thus providing opportunities for saltwater intrusion and dissolution once the blocks were exposed to saltwater conditions. The dissolution of PG increases the concentration of sulfate ions that can react with calcium aluminum oxides in class C fly ash to form additional ettringite, thus accelerating rupture development. Within these ruptures, the solution could easily reach its saturated state, allowing for the re-crystallization of gypsum on the class C fly ash particle surface, which was observed in the SEM images. Even though $CaCO_3$ was formed on the PG composite surfaces, the ruptures were too substantial, and $CaCO_3$ could not prevent the composites from saltwater intrusion. Eventually, the PG:class C fly ash:lime composites completely dissolved in the saltwater.

The results obtained in this study differ from those of other investigators. Hockley and Sloot [33] investigated the use of fly ash:flue gas desulfurization (FGD) sludge:cement:lime

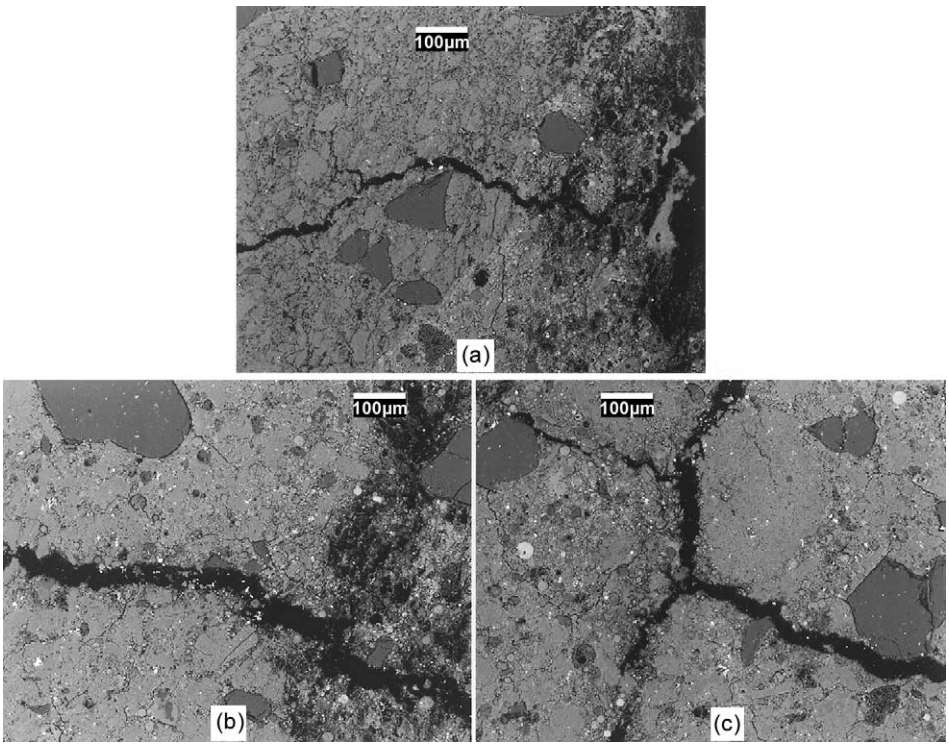

Fig. 9. BS images of the PG composite surface zone after 28 days saltwater dynamic leaching test showed rupture development. (a) 62%:35%:3% PG:class C fly ash:lime. (b) 55%:42%:3% PG:class C fly ash:lime. (c) 58.5%:35%:6.5% PG:class C fly ash:lime.

blocks in marine environments. These composites, which survived in saltwater for 8 years, contained calcium carbonate and magnesium hydroxide precipitates in the pores of the block surface, protecting the composites from degradation. One major difference between this study and Hockley and Sloot [33] was the surface area to volume ratio of the test composites. The PG:class C fly ash:lime composites had a specific surface area (SSA) of 4 cm^2 cm^{-3}, while the fly ash:FGD:lime:cement had a SSA of approximately 0.81 cm^2 cm^{-3}. Thus, the PG composites had much more exposed surface area for degradation to occur.

The key parameter in this study was lime. As discussed earlier, when the lime content increased, the percent diametrical expansion also increased neutralizing the benefit of any $CaCO_3$ that may have formed on the surface. The minimum lime content used for this study was 3%, all in the active form. In previous studies with PG:fly ash:cement, the maximum content of cement was 10%, which is equivalent to 3.3% hydrated lime [11]. However, some of this hydrated lime is concealed by the cement paste and is not active. The high active lime content (>3%) in the PG:class C fly ash:lime composites resulted in greater percent diametrical expansions and wider ruptures (Eqs. (12) and (13)). The field saltwater submergence experiments showed that PG:class C fly ash:lime composites with lime content

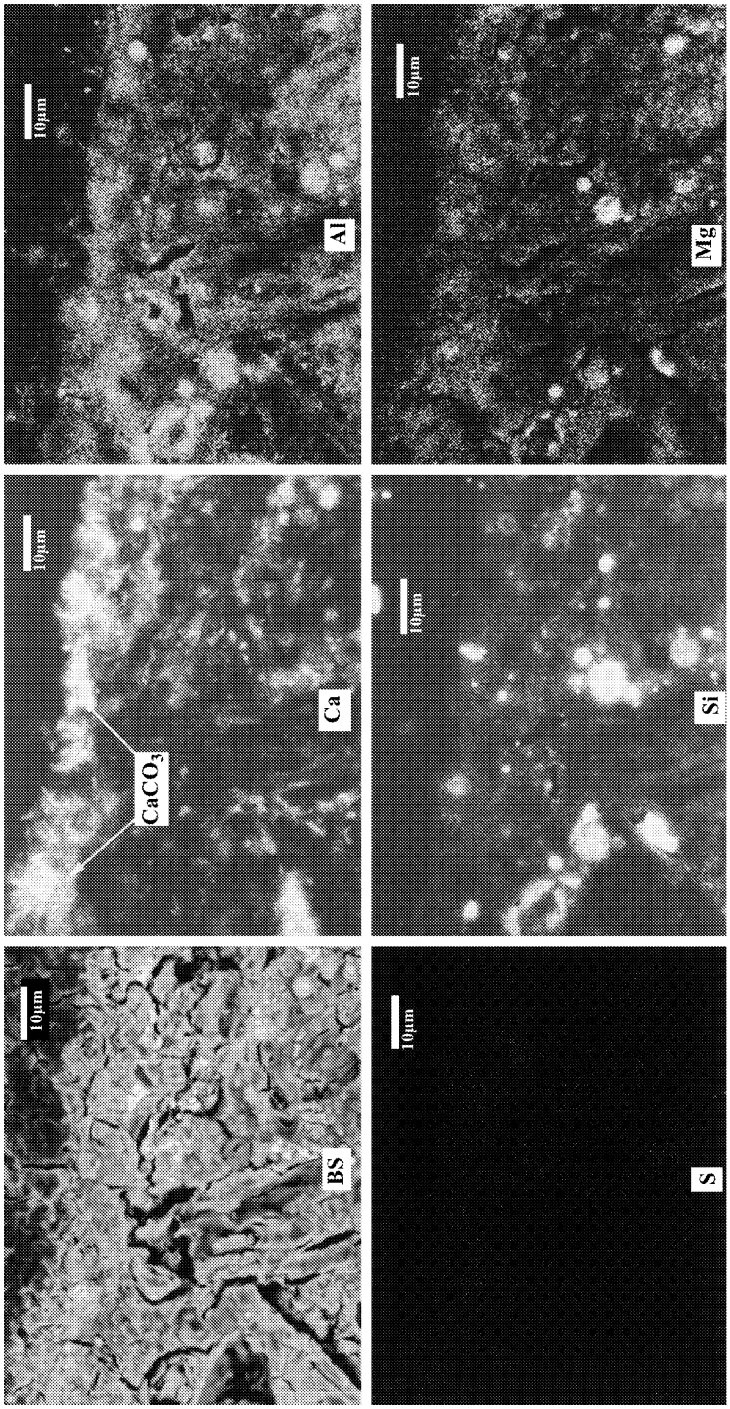

Fig. 10. Elemental content and BS images of 62%:35%:3% PG:class C fly ash:lime composite showed $CaCO_3$ coating formation.

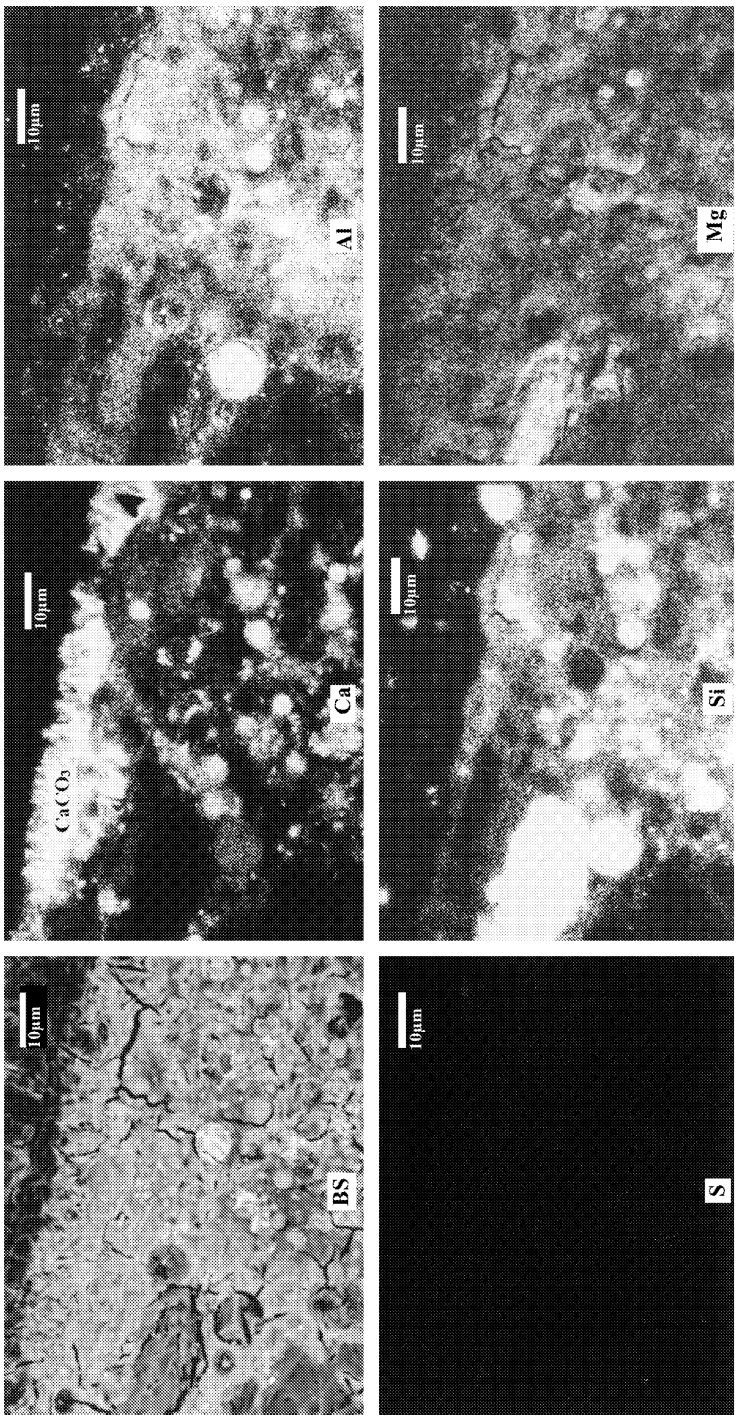

Fig. 11. Elemental content and BS images of 58.5%:35%:6.5% PG:class C fly ash:lime composite showed $CaCO_3$ coating formation.

Table 4
Effective diffusion coefficients and effective diffusion depths ($t = 30$ years) were calculated for the composites subjected to the 28 days dynamic leaching study

PG (%)	Class C fly ash (%)	Lime (%)	C_0 ($\times 10^{-6}$, mol l^{-1})	D_e ($\times 10^{-13}$, m^2 s^{-1})	Mean D_e ($\times 10^{-13}$, m^2 s^{-1})	X_c (mm)	Mean X_c (mm)
62.0	35.0	3.0	6.43	2.31	2.12	20.9	20.0
62.0	35.0	3.0	6.43	1.92	–	19.1	–
58.5	38.5	3.0	6.11	2.33	2.23	21.0	20.5
58.5	38.5	3.0	6.11	2.13	–	20.1	–
55.0	42.0	3.0	5.79	1.88	2.02	18.9	19.6
55.0	42.0	3.0	5.79	2.16	–	20.2	–
59.6	36.2	4.2	6.52	1.96	2.61	19.3	22.1
59.6	36.2	4.2	6.52	3.26	–	24.8	–
56.2	39.6	4.2	6.21	3.43	3.14	25.5	24.3
56.2	39.6	4.2	6.21	2.85	–	23.2	–
57.4	37.3	5.3	6.59	2.10	2.64	20.0	22.3
57.4	37.3	5.3	6.59	3.18	–	24.6	–
58.5	35.0	6.5	7.00	2.70	2.33	22.6	20.9
58.5	35.0	6.5	7.00	1.95	–	19.2	–
55.0	38.5	6.5	6.68	1.24	1.40	15.3	16.2
55.0	38.5	6.5	6.68	1.56	–	17.2	–
56.2	36.2	7.6	7.06	1.52	1.37	17.0	16.1
56.2	36.2	7.6	7.06	1.21	–	15.1	–
55.0	35.0	10.0	7.56	0.964	1.15	13.5	14.7
55.0	35.0	10.0	7.56	1.33	–	15.9	–

greater than 3% could not survive in the saltwater environment, irrespective of the low calcium diffusion coefficients, which were comparable to other solid waste studies in which the stabilized waste blocks did survive natural saltwater conditions for extended periods [12,26].

The effective diffusion coefficients obtained during this study are the same order of magnitude as stabilized FGD:fly ash blocks ($(0.83–2.2) \times 10^{-13}$ m^2 s^{-1}) [26]. Effective diffusion depths (14.7–24.3 mm) calculated for $t = 30$ years while slightly higher, were also the same magnitude as those obtained for fly ash:FGD:lime:cement blocks (2.0–11.9 mm) [26]. Based on D_e and X_c, it seems that both PG:class C fly ash:lime composite and fly ash:FGD:lime:cement blocks should behave similarly. However, the saltwater submergence experiments results varied drastically (Table 4). The fly ash:FGD:lime:cement composites survived in saltwater for more than 2 years, while PG:class C fly ash:lime composites survived for only 15 weeks. Therefore the effective diffusion coefficients and effective diffusion depths cannot be used as an indicator of long-term survivability of the solid waste if the composite contains multiple ruptures. The effective diffusion coefficients and effective diffusion depths can be used as an indicator of the long-term survivability in saltwater conditions if diffusion is the sole process contributing to the loss of ions and the composite contains no rupture. These conditions were observed for PG:class C fly ash:Portland type II cement composites [29] and fly ash:FGD:lime:cement blocks [26].

This research has brought to light that diffusion coefficients used independently of other characterizing parameters are not good indicators of the potential long-term survivability of

stabilized solid waste composites in natural saltwater environments. Other mitigating factors including saltwater intrusion, specific surface and rupture development must be taken into consideration. The data clearly suggest that PG:class C fly ash:lime composites with lime content >3% do not have a long-term survivability potential within marine environments.

Acknowledgements

This research was supported by the Florida Institute of Phosphate Research (Contract #95-01-127). The SEM and EDS were performed in the SEM and Microanalysis Laboratory, Department of Geology, Louisiana State University. The authors thank Dr. Xiaogang Xie and Mr. Rick Young for their support in analyzing the samples. The authors thank Miss Autumn S. Hawke for her help in data analysis. The authors thank Sarah Jones for reviewing this manuscript.

References

[1] R. Taha, R.K. Seals, Phosphogypsum Literature Review, A Report by the Institute of Recyclable Materials to Freeport McMoRan, Louisiana State University, Louisiana, 1991.
[2] USEPA, http://www.epa.gov/radiation/neshaps/subpartr/more.htm, 2000.
[3] Idaho State University, The Radiation Information Network, Radioactivity in Nature, http://www.physics.isu.edu/radinf/natural.htm, 2001.
[4] USEPA, http://www.epa.gov/ttn/uatw/hlthef/radionuc.html, 2001.
[5] Federal Register, Vol. 64, No. 22, 40 CFR Part 61, Subpart 61, 3 February 1999, pp. 5573–5580.
[6] Federal Register, 40 CFR Part 61, Subpart I, 15 December 1989.
[7] Florida Institute of Phosphate Research, Strategic Indicators of Success, March 1996.
[8] USEPA, Report to Congress on Special Wastes from Mineral Processing, Solid Waste and Emergency Response, EPA/503-sw-90-070c, 1990.
[9] S. Chen, K.A. Rusch, R.F. Malone, R.K. Seals, C.A. Wilson, J.W. Fleeger, Preliminary evaluation of stabilized phosphogypsum for use within the aquatic environment, in: Proceedings of the Water Environment Federation, Special Workshop on Food Chain Toxicity—Toxic Substances in Water Environmental: Assessment and Control, 14–17 May 1995, Cincinnati, OH.
[10] C.A. Wilson, W.R. Keithly, Final Report: Economic Analysis of the Use of PG/Fly Ash/Portland Type II Cement for Enhancement of Fisheries Habitat, FIPR Contract #95-01-127, Coastal Fisheries Institute, Center for Coastal, Energy, and Environmental Resources Louisiana State University, Louisiana, 1999, pp. 55–70.
[11] T. Guo, Determination of Optimal Composition of Stabilized Phosphogypsum Composites for Saltwater Application, Ph.D. Dissertation, Louisiana State University, Louisiana, 1998, pp. 137–138.
[12] T. Guo, R.K. Seals, R.F. Malone, K.A. Rusch, Environ. Eng. Sci. 16 (1999) 147–156.
[13] T. Guo, A.S. Hawke, K.A. Rusch, Environ. Sci. Technol. 33 (1999) 3185–3191.
[14] A.N. James, Soluble Materials in Civil Engineering, Ellis Horwood Limited, Market Cross House, England, 1992.
[15] T. Guo, R.F. Malone, K.A. Rusch, Environ. Sci. Technol. 35 (2001) 3967–3973.
[16] A. Atalay, J.G. Laguros, in: Proceedings of the Material Research Society Symposium, Vol. 178, Boston, MA, 1989, pp. 261–266.
[17] F.P. Glasser, S. Diamond, D.M. Roy, in: Proceedings of the Material Research Society Symposium, Vol. 86, Boston, MA, 1986, pp. 139–158.
[18] R.I.A. Malek, D.M. Roy, in: Proceedings of the Material Research Society Symposium, Vol. 113, Boston, MA, 1987, pp. 133–144.
[19] K. Hinkelmann, O. Kempthorne, Design and analysis of experiments, Instruction to Experimental Design, Vol. 1, Wiley, New York, 1994.

[20] P.O. Kuehl, Statistical Principles of Research Design and Analysis, Duxbury Press, Belmont, 1994.
[21] C.S. Gutti, R.J.B. Metcalf, R.K. Seals, Cement Concrete Res. 26 (1996) 1083–1094.
[22] A.M. Neville, Properties of Concrete, 4th Edition, Longman Group Limited, England, 1995, p. 72.
[23] ANS, Measurements of the Leachability of Solidified Low-Level Radioactive Wastes, ANSI/ANS 16.1, American Nuclear Society, La Grandge Park, IL, 1986.
[24] Eaton, Clesceri, Greenburg (Eds.), Standard Methods for Examination of Water and Wastewater, 20th Edition, American Public Health Association (APHA), American Waterworks Association, and Water Environment Federation, Washington, DC, 1998.
[25] C.D. Shackelford, D.E. Daniel, J. Geotech. Eng., ASCE 117 (1991) 467–484.
[26] I.W. Duedall, J.S. Buyer, M.G. Heaton, S.A. Oakley, A. Okubo, R. Dayal, M. Tatro, F.J. Roeththel, R.J. Wilke, J.P. Hershey, Diffusion of calcium and sulfate ions in stabilized coal wastes, in: I.W. Duedall, B.H. Ketchum, P.K. Park, D.R. Kester (Eds.), Wastes in the Ocean: Industrial and Sewage Wastes in the Ocean, Vol. 1, Wiley/Interscience, New York, 1983, pp. 375–395.
[27] P. Cote, Contaminant Leaching from Cement-Based Waste Forms Under Acid Conditions, Ph.D. Thesis, McMaster University, Toronto, 1996.
[28] J.L. Seveque, M.D. Cayeux, E.H. Nouguier, Cement and Concrete 22 (1992) 477–488.
[29] C.S. Hutchinson, Laboratory Handbook of Petrographic Techniques, Wiley, New York, 1974.
[30] A. Roy, R. Kavakaalva, R.K. Seals, ASCE J. Mater. Civil Eng. 8 (1996) 11–88.
[31] L.J. Minnick, Reactions of hydrated lime with pulverized coal fly ash, in: Proceedings of the Fly Ash Utilization Conference, Bureau of Mines Information Circular 8348, 1967.
[32] R.E.J. Ferrell, A. Arman, G. Baykal, in: Proceedings of the Material Research Society Symposium, Vol. 113, Boston, MA, 1987, pp. 241–248.
[33] D.E. Hockley, H.A. Sloot, Environ. Sci. Technol. 25 (1991) 1408–1414.